ARR No. 3E10

NATIONAL ADVISORY COMMITTEE FOR AERONAUTICS

WARTIME REPORT

ORIGINALLY ISSUED

May 1943 as
Advance Restricted Report 3E10

AN INVESTIGATION OF AIRCRAFT HEATERS

XII - PERFORMANCE OF A FORMED-PLATE CROSSFLOW EXHAUST GAS AND AIR HEAT EXCHANGER

By L. M. K. Boelter, H. G. Dennison,
A. G. Guibert, and E. H. Morrin
University of California

NACA

WASHINGTON

NATIONAL ADVISORY COMMITTEE FOR AERONAUTICS

ADVANCE RESTRICTED REPORT

AN INVESTIGATION OF AIRCRAFT HEATERS

XII - PERFORMANCE OF A FORMED-PLATE CROSSFLOW EXHAUST GAS AND AIR HEAT EXCHANGER

By L. M. K. Boelter, H. G. Dennison,
A. G. Guibert, and E. H. Morrin

SUMMARY

Performance data on a Trane exhaust gas and air heat exchanger are presented. Heat transfer rates were measured using exhaust gas rates ranging from 4550 lb/hr to 7000 lb/hr and ventilating-air rates from 2200 lb/hr to 4750 lb/hr. The inlet exhaust gas temperature was maintained at approximately 1400° F; whereas the inlet temperature of the ventilating air was about 95° F. Pressure drop measurements were made across the exhaust-gas side and across the ventilating air side of the heat exchanger under isothermal and non-isothermal conditions. In addition, isothermal pressure drops across the inlet and outlet air ducts alone were measured.

The maximum measured rate of heat transfer was 369,000 Btu/hr with maximum static pressure drops of 18.8 inches of water and 13.9 inches of water on the exhaust gas and ventilating air sides of the heat exchanger, respectively.

The measured thermal outputs and the static pressure drops are compared with predicted magnitudes.

INTRODUCTION

The heater was tested on the large test stand in the Mechanical Engineering Laboratories of the University of California. (See photograph (fig. 1) and a description of this test stand in reference 1.) This heater was designed for use in the exhaust gas system of aircraft engines for the purpose of supplying heated air to the cabin, the wing, and the tail surfaces.

The following data were obtained:

1. Weight rates of exhaust gas and ventilating air through the two sides of the heat exchanger

2. Temperatures of ventilating air and of exhaust gas at entrance and exit of the heater

3. Temperatures of the heater surfaces

4. Static pressure drop measurements on the exhaust gas and ventilating air sides of the heater under both isothermal and non-isothermal flow conditions

5. Isothermal static pressure drop measurements across the air inlet and outlet ducts

DESCRIPTION OF THE TRANE HEATER AND OF THE TESTING PROCEDURE

The trane heater is an all-prime-surface crossflow unit consisting of alternate ventilating air and exhaust gas passages made from preformed sheets about $13\frac{3}{4}$ by $7\frac{1}{4}$ inches. The passages on the exhaust gas side, 56 in number, are straight diamond-shape channels $13\frac{3}{4}$ inches in length, On the ventilating air side, there are 15 zigzag passages of rectangular cross section and a length of $6\frac{1}{2}$ inches the sinuous passages of which conform to the contours of the exhaust gas passages. The sheets are mounted in a frame of light angle iron, forming a unit with over-all dimensions of approximately $14\frac{1}{4}$ by $8\frac{1}{2}$ by $8\frac{1}{2}$ inches. A sketch of the heat exchanger is shown in figure 7. Also, photographs of the heater are shown in figures 2 to 4. The inlet duct of the air shroud contained vanes arranged to distribute the flow of ventilating air across the heater.

The weight rates of exhaust gas and ventilating air were obtained by means of calibrated square-edge orifices.

The exhaust gas temperatures were measured at the inlet and outlet of the heater by means of shielded traversing thermocouples. Unshielded traversing thermocouples were used to measure the temperature of the ventilating air.

A mixing device was used at the exit of the natural-gas furnace to improve the temperature distribution at the entrance to the heater. The temperature distributions (in deg. F)-were as follows:

Exhaust gas inlet ±7 percent of complete uniformity

Exhaust gas outlet ±2 percent of complete uniformity

Ventilating air outlet $\pm 1\frac{1}{2}$ percent of complete uniformity

Ventilating air inlet (complete uniformity)

The traversing thermocouples were installed at the following points:

Exhaust gas inlet temperature traverse - 15 inches upstream from heater

Exhaust gas outlet temperature traverse - $24\frac{1}{2}$ inches downstream from heater

Ventilating air inlet temperature traverse - 7 inches upstream from heater

Ventilating air outlet temperature traverse - 34 inches downstream from heater

The heat loss to the surroundings was reduced to a negligible amount by wrapping the ducts and the heater with asbestos sheets.

Temperatures of the heater surfaces were measured at six points, three on each side (ventilating air inlet and outlet sides) of the heater. (See figs. 2 and 3.)

Static pressure drop measurements were made across the ventilating air and exhaust gas sides of the heater. Two taps, 180° apart, were installed at each pressure-measuring station. The pressure taps on the 8-inch exhaust gas ducts were placed $5\frac{1}{2}$ inches upstream and 7 inches downstream from the heat transfer section of the heater; whereas those on the ventilating air side were placed in a 5-inch duct $11\frac{1}{2}$ inches upstream and 14 inches downstream from the air shroud openings.

Isothermal static pressure drop measurements across the air inlet and outlet ducts alone were made by separating these ducts by a "spacer" equivalent to the heater width, so that the ducts were in positions corresponding to those for measurements across the ducts and the heater. The pressure drop in the "spacer" was computed and found to be negligibly small.

SYMBOLS

A area of heat transfer, ft^2

A_a total cross-sectional area of the passages on the ventilating air side of the heater, ft^2

A_g total cross-sectional area of the passages on the exhaust gas side of the heater, ft^2

A_1 cross-sectional area of the inlet and outlet exhaust gas ducts, ft^2

A_2 total cross-sectional area at the tapered ends of the exhaust gas passages, ft^2

A_3 cross-sectional area of the ventilating air outlet duct, ft^2

c_{p_a} heat capacity of air at constant pressure, Btu/lb °F

c_{p_g} heat capacity of exhaust gas at constant pressure, Btu/lb °F

D hydraulic diameter, ft

D_a hydraulic diameter on ventilating air side, ft

D_g hydraulic diameter on exhaust gas side, ft

f_c unit thermal convective conductance (average with length), Btu/hr ft^2 °F

f_{c_a} unit thermal convective conductance for the ventilating air (average with length), Btu/hr ft^2 °F

f_{c_g} unit thermal convective conductance for the exhaust gas (average with length), Btu/hr ft^2 °F

g	gravitational force per unit of mass, lb/(lb sec^2/ft)
G	weight rate per unit of area, lb/hr ft^2
G_a	weight rate per unit of area for ventilating air, lb/hr ft^2
G_g	weight rate per unit of area for exhaust gas, lb/hr ft^2
K	coefficient for isothermal pressure drop due to gradual contraction of fluids
K_c	coefficient for isothermal pressure drop due to sudden contraction of fluids
L	length of fluid passages; also length of heat transfer surface, ft
q_a	measured rate of enthalpy change of ventilating air, Btu/hr
q_g	measured rate of enthalpy change of exhaust gas, Btu/hr
t_a	arithmetic average of three surface temperature measurements taken near the ventilating air inlet, °F
t_b	arithmetic average of three surface temperature measurements taken near the ventilating air outlet, °F
T_a	arithmetic average mixed-mean absolute temperature of ventilating air $= \dfrac{{}^{T}a_1 + {}^{T}a_2}{2} + 460$, °R
T_{av}	arithmetic average mixed-mean absolute temperature of fluid $= \dfrac{T_1 + T_2}{2}$, °R
T_g	arithmetic average mixed-mean absolute temperature of exhaust gas $= \dfrac{{}^{T}g_1 + {}^{T}g_2}{2} + 460$, °R
T_1	mixed-mean absolute temperature of fluid at entrance section (point 1), °R
T_2	mixed-mean absolute temperature of fluid at exit section (point 2), °R

T_{iso} mixed-mean absolute temperature of fluid for isothermal pressure drop tests, °R

u_m mean velocity of fluid at minimum cross-sectional area of fluid passages, ft/sec

U over-all unit thermal conductance, Btu/hr ft^2 °F

UA over-all thermal conductance, Btu/hr °F

W weight rate of fluid, lb/hr

W_a weight rate of air, lb/hr

W_g weight rate of exhaust gas, lb/hr

γ_1 weight density of fluid at entrance to heating section (point 1), lb/ft^3

ΔP pressure drop along heater, lb/ft^2

ΔP_a pressure drop along heater on ventilating air side, lb/ft^2

$\Delta P'_a$ pressure drop along heater on ventilating air side, inches H_2O

ΔP_g pressure drop along heater on exhaust gas side, lb/ft^2

$\Delta P'_g$ pressure drop along heater on exhaust gas side, inches H_2O

ΔP_{contr} isothermal pressure drop due to contraction, lb/ft^2

ΔP_{duct} isothermal pressure drop along inlet and outlet ducts of the air shroud, lb/ft^2

ΔP_{exp} isothermal pressure drop due to expansion, lb/ft^2

ΔP_{fric} isothermal pressure drop due to friction, lb/ft^2

$\Delta P_{T_{iso}}$ isothermal pressure drop along heater and ducts at temperature T_{iso}, lb/ft^2

ζ_{iso} isothermal friction factor defined by $\frac{\Delta P}{\gamma} = \zeta_{iso}\frac{L}{D}\frac{u_m^2}{2g}$

Δt_{lm} logarithmic mean temperature difference, °F

$\Delta\tau_a$ difference between mixed-mean temperatures of ventilating air at sections defined by points 1 and 2 = $\tau_{a_2} - \tau_{a_1}$, $^{\circ}F$

$\Delta\tau_g$ difference between mixed-mean temperatures of exhaust gas at sections defined by points 1 and 2 = $\tau_{g_1} - \tau_{g_2}$, $^{\circ}F$

μ viscosity of fluid, lb sec/ft^2

τ_{a_1} mixed-mean temperature of ventilating air at entrance section (point 1), $^{\circ}F$

τ_{a_2} mixed-mean temperature of ventilating air at exit section (point 2), $^{\circ}F$

τ_{g_1} mixed-mean temperature of exhaust gas at entrance section (point 1), $^{\circ}F$

τ_{g_2} mixed-mean temperature of exhaust gas at exit section (point 2), $^{\circ}F$

Nu Nusselt number = $\dfrac{f_c D}{k}$

Pr Prandtl number = $\dfrac{\mu\, c_p}{k}\, 3600\, g$

Re Reynolds number = $\dfrac{G\, D}{3600\, \mu\, g}$

METHOD OF ANALYSIS

Heat Transfer

The thermal output of the heater was determined by the enthalpy change of the ventilating air:

$$q_a = W_a\, c_{p_a}(\tau_{a_2} - \tau_{a_1}) \tag{1}$$

in which c_{p_a} was evaluated at the arithmetic average ventilating air temperature as a good approximation. A plot of q_a against W_a at constant values of the exhaust gas rate W_g is shown in figure 8.

On the exhaust gas side of the heater:

$$q_g = W_g \, c_{p_g}(T_{g_1} - T_{g_2}) \tag{2}$$

where c_{p_g} was evaluated for air at the arithmetic average exhaust gas temperature.

The measured over-all thermal conductance UA was evaluated from the expression:

$$q_a = (UA)\Delta t_{lm} \tag{3}$$

The value of Δt_{lm} for crossflow is chosen as that for counterflow and then multiplied by a correction factor. (See reference 2, p. 147.) Inasmuch as this correction factor was always within 1 percent of unity, the Δt_{lm} used in these calculations was taken to be that for counterflow of the fluids.

A plot of UA as a function of the ventilating air rate W_a at constant values of W_g is shown in figure 9. The thermal output of the heater for values of Δt_{lm} other than those used here may be predicted by determining UA at the corresponding weight rates from figure 9 and using these magnitudes in equation (3).

The predicted rate of heat transfer plotted in figure 9 was calculated by means of the equation

$$UA = \frac{1}{\left(\frac{1}{f_c A}\right)_a + \left(\frac{1}{f_c A}\right)_g} \tag{4}$$

where A is the heat transfer area, and the unit thermal conductances f_{c_a} and f_{c_g}, on the ventilating air and exhaust gas sides of the heater, respectively, are evaluated from the following equations:

$$f_{c_a} = 5.56 \times 10^{-4} T_a^{\,0.296} \frac{G_a^{\,0.8}}{D_a^{\,0.2}} \tag{5}$$

and

$$f_{c_g} = 5.56 \times 10^{-4} \, T_g^{0.296} \frac{G_g^{0.8}}{D_g^{0.2}} \qquad (6)$$

where D is the hydraulic diameter and the subscripts a and g refer to the ventilating air and exhaust gas sides, respectively. (See reference 3, equations (16) and (17), for derivation of equations (5) and (6).)

Pressure Drop

Measurements of the static pressure drops across the air and gas sides of the heater were made under isothermal and non-isothermal conditions. A determination of the pressure drops across the air inlet and outlet ducts alone under isothermal conditions also was made. The isothermal pressure drop across the heater alone ΔP_{htr} was determined by the difference between the measured drop across both ducts and heater $\Delta P_{T_{iso}}$ and that across the ducts alone ΔP_{duct}.

These data were employed to evaluate the isothermal friction factor ζ_{iso} for the <u>air side</u> of the heater by means of the expressions

$$\Delta P_{T_{iso}} - \Delta P_{duct} = \Delta P_{htr} = \Delta P_{contr} + \Delta P_{frict} + \Delta P_{exp} \qquad (7)$$

The <u>contraction</u> loss is obtained from

$$\Delta P_{contr} = K_c \, \gamma \frac{u_m^2}{2g} \qquad (8)$$

in which u_m is the mean velocity in the air passages of the heater and γ is the unit weight of the air, evaluated at T_{iso}. The magnitude of K_c was obtained from reference 4 or reference 5 ($K_c = 0.30$).

The <u>frictional</u> pressure drop is evaluated from

$$\Delta P_{frict} = \zeta_{iso} \frac{L}{D} \frac{u_m^2}{2g} \qquad (9)$$

and the expansion loss is obtained from

$$\Delta P_{exp} = \gamma \frac{u_m^2}{2g} \left(1 - \frac{A_a}{A_3} \right)^2 \qquad (10)$$

where A_a is the cross-sectional area of the air side of the heater and A_3 is the cross-sectional area of the outlet air duct. Thus ζ_{iso} is obtained from

$$\frac{\Delta P_{htr}}{\gamma} = \frac{u_m^2}{2g} \left[\left(1 - \frac{A_a}{A_3} \right)^2 + K_c + \zeta_{iso} \frac{L}{D} \right] \qquad (11)$$

Magnitudes of ζ_{iso} evaluated from this equation are given in table II.

For the gas side, the measured isothermal static pressure drop $\Delta P_{T_{iso}}$ was that across the heater alone; so $\Delta P_{htr} = \Delta P_{T_{iso}}$. The gas passages were slightly tapered on each end so that the isothermal pressure drop consisted of the following five terms:

a) A sudden contraction from gas-inlet duct to entrance end of gas passages

b) A gradual contraction along tapered entrance to passages up to point of minimum cross-sectional area

c) The frictional pressure drop through center section of passages at minimum cross-sectional area

d) A gradual expansion at tapered ends of passages

e) A sudden expansion from end of passages into gas-outlet duct

The expression for the isothermal pressure drop due to these five terms is then written in a form similar to equations (7) and (11):

$$\frac{\Delta P_{htr}}{\gamma} = \frac{u_m^2}{2g} \left[\left(\frac{A_g}{A_2} \right)^2 K_c + K + \zeta_{iso} \frac{L}{D} + (1 - \eta) \left[1 - \left(\frac{A_g}{A_2} \right)^2 \right] + \left(\frac{A_g}{A_2} \right)^2 \left[1 - \left(\frac{A_2}{A_1} \right) \right]^2 \right] \qquad (12)$$

in which $K_c = 0.14$, the coefficient for sudden contraction, is obtained from reference 4 or reference 5; $K = 0.04$, the coefficient for gradual contraction, also is obtained from reference 4 or reference 5; $(1 - \eta) = 0.25$, the coefficient for gradual expansion, is obtained from reference 6; and the last term on the right side of equation (12) is the same as equation (10) for sudden expansion losses. The cross-sectional area A_1 is that of the inlet and outlet exhaust gas ducts; A_2 is the total area at the ends of the gas passages; and A_g is the minimum area at the center of the passages which is the total cross-sectional area on the exhaust-gas side of the heater used also in equation (6) for the computation of the unit thermal conductance, f_{c_g}. Thus, ζ_{iso} is calculated by means of equation (12) from the measured pressure drop across the heater alone ΔP_{htr}. Calculated values of ζ_{iso} are compared to predicted values taken for a smooth pipe. (See fig. 7 of reference 7.)

The non-isothermal pressure drop of either fluid through the heat exchanger was predicted from isothermal measurements by means of equation (6) of reference 1.

$$\Delta P = \Delta P_{T_{iso}} \left(\frac{T_{av}}{T_{iso}}\right)^{1.13} + \left(\frac{G}{3600}\right)^{2} \frac{1}{\gamma_1 g} \left(\frac{T_2}{T_1} - 1\right) \qquad (13)$$

where

$\Delta P_{T_{iso}}$ total measured isothermal pressure drop (due to friction alone) at temperature T_{iso}

T_1 and T_2 mixed-mean absolute temperatures of fluid at inlet and outlet of heater, respectively

T_{av} arithmetic average of T_1 and T_2

G fluid flow per unit cross-sectional area

γ_1 unit weight, evaluated at temperature T_1, of fluid at inlet to heater

A comparison of measured and predicted non-isothermal pressure drops across each side of the heater is presented in table IV and is shown graphically in figures 10 and 11.

Heat transfer and pressure drop data for this Trane heat exchanger are presented in table I.

DISCUSSION

The arithmetic average of all the heat balance ratios (q_g/q_a) was 0.975. The improvement over the ratios found in tests on other heaters was due to the better temperature distribution attained at the exhaust gas outlet of this heater. The exhaust gas experienced a sudden expansion from the tubes of the heater into the outlet ducts, and also "central cores of hot gas," encountered in many heaters, were absent in this case because of the great number of exhaust gas passages.

The magnitudes of the over-all thermal conductance UA predicted by means of equations (4), (5), and (6) are about 10 percent lower than the values obtained from laboratory data at an air rate of 5000 lb/hr and about 25 percent lower at an air rate of 2000 lb/hr. The use of the multiplier $(1 + 1.1\ D/L)$ in equations (5) and (6) to account for the higher unit thermal conductance near the entrance of a tube or channel would yield magnitudes of UA about 5 percent higher than those which were obtained from equations (5) and (6) upon neglect of this correction. (See Appendix of reference 8.) Also the sinuous character of the passages on the air side of the heater may actually increase the unit thermal conductance over that expressed by equation (5), which is based on results of straight tubes.

The predicted unit thermal conductance on the gas side of the heater was found to be much larger than that on the air side. Thus, the controlling resistance to heat transfer was on the air side. It may be possible, therefore, to re-proportion the air and gas cross-sectional areas in order to reduce the large static pressure drop on the exhaust gas side but not reduce appreciably the thermal output of the heater. The temperature of the heater surfaces would thus also be diminished.

The isothermal friction factor along the air side of the heater alone, computed from laboratory pressure drop measurements, is larger than would be predicted for smooth or even rough pipes or channels. This fact may have been due to eddies caused by the zigzag path followed by the ventilating air as it passed through the heater. The isothermal pressure drop through the inlet and outlet air ducts was about 30 percent of the total drop across the ducts and the heater. (See table II.)

The isothermal friction factor along the exhaust gas side of the heater computed from laboratory pressure drop measurements by means of equation (12) was within 7 percent of the predicted value for a smooth tube.

Magnitudes of $f_{iso} \frac{L}{D}$ are also tabulated in tables II and III. A comparison of these values with those of a slotted-fin heater (see reference 9, tables VII and VIII) reveals that $f_{iso} \frac{L}{D}$ for either type of heater is approximately 0.7 for the exhaust gas sides and approximately 2.5 for the ventilating air sides. These values are, of course, a function of the weight rate per unit of cross-sectional area G. The higher values of this ratio on the air side may be explained by the turbulence- or eddy-forming path usually followed by the ventilating air.

The values of the non-isothermal pressure drop across the heater predicted from the measured isothermal drop by means of equation (13) compare well with the values measured in the laboratory. (See figs. 10 and 11 and table IV.) The slope of the non-isothermal pressure drop curve should be greater than the slope for the isothermal curve for the cooling exhaust gases; whereas it should be less in the case of the heated ventilating air. An inspection of equation (13) reveals the basis for these effects.

The heater tested here was constructed of 1/32-inch iron sheets and weighed 33 pounds. It is believed that a similar heater has been made of thinner metal by the same firm, thus considerably reducing the weight of the unit.

CONCLUSIONS

1. The thermal output of the Trane heater at an air rate of 3000 lb/hr and an exhaust gas rate of 5800 lb/hr was 285,000 Btu/hr. The pressure drops, under these conditions, were 6.2 inches of water on the air side and 14 inches of water on the exhaust gas side.

2. It may be possible to reduce the large pressure drop on the exhaust gas side by reducing the restriction in the cross-sectional area and yet not greatly reduce the thermal output of the heater, because the controlling resistance to heat transfer appears to be on the ventilating air side.

3. The thermal output of this heater may be predicted within 10 to 25 percent by means of equations (3) to (6). The sinuosity of the air-side passages may account for part of the discrepancy between the predicted and measured magnitudes of the over-all thermal conductance UA. The air-side pressure drop also is probably affected.

4. The thermal performance using fluid temperatures other than those used in the tests reported herein can be predicted by obtaining the over-all thermal conductance UA from figure 9 at the actual fluid rates and substituting in equation (3).

5. The isothermal pressure drop on the exhaust gas side of the heater can be predicted using a friction factor for a smooth tube in equation (12).

University of California,
Berkeley, Calif.

REFERENCES

1. Boelter, L. M. K., Miller, M. A., Sharp, W. H., Morrin, E. H., Iverson, H. W., and Mason, W. E.: An Investigation of Aircraft Heaters. IX - Measured and Predicted Performance of Two Exhaust Gas-Air Heat Exchangers and an Apparatus for Evaluating Exhaust Gas-Air Heat Exchangers. NACA A.R.R., March 1943.

2. McAdams, W. H.: Heat Transmission. McGraw-Hill Book Co., Inc., New York, N. Y., 2d ed., 1942, p. 147.

3. Martinelli, R. C., Weinberg, E. B., Morrin, E. H., and Boelter, L. M. K.: An Investigation of Aircraft Heaters. III - Measured and Predicted Performance of Double Tube Heat Exchangers. NACA A.R.R., Oct. 1942, equations (16) and (17).

4. O'Brien, M. P., and Hickox, G. H.: Applied Fluid Mechanics. McGraw-Hill Book Co., Inc., New York, N. Y., 1937, pp. 211-213.

5. Dodge, R. A., and Thompson, M. J.: Fluid Mechanics. McGraw-Hill Book Co., Inc., New York, N. Y., 1937, pp. 215-216.

6. Patterson, G. M.: Modern Diffuser Design Aircraft Engineering, London, England, vol. X., no. 115, Sept. 1938, p. 267.

7. Martinelli, R. C., Weinberg, E. B., Morrin, E. H., and Boelter, L. M. K.: An Investigation of Aircraft Heaters. IV - Measured and Predicted Performance of Longitudinally Finned Tubes. NACA A.R.R., Oct. 1942, fig. 7.

8. Boelter, L. M. K., Dennison, H. G., Guibert, A. G., and Morrin, E. H.: An Investigation of Aircraft Heaters. X - Measured and Predicted Performance of a Fluted-Type Exhaust Gas and Air Heat Exchanger. NACA A.R.R., March 1943.

9. Boelter, L. M. K., Miller, M. A., Sharp, W. H., and Morrin, E. H.: An Investigation of Aircraft Heaters. XI - Measured and Predicted Performance of a Slotted-Fin Exhaust Gas and Air Heat Exchanger. NACA A.R.R., April 1943, tables VII and VIII.

TABLE I.- EXPERIMENTAL RESULTS ON TRANE CROSS-FLOW HEATER

Run	AIR SIDE						EXHAUST-GAS SIDE							HEATER TEMPS.		OVERALL PERFORMANCE	
Run	T_{a_1}	T_{a_2}	ΔT_a	W_a	$\Delta P_a'$	q_a	T_{g_1}	T_{g_2}	ΔT_g	W_g	$\Delta P_g'$	q_g	$\frac{q_g}{q_a}$	t_a	t_b	Δt_{lm}	(UA)
No.	°F	°F	°F	$\frac{lb}{hr}$	Inches H_2O	$\frac{KBtu}{hr}$	°F	°F	°F	$\frac{lb}{hr}$	Inches H_2O	$\frac{KBtu}{hr}$		°F	°F	°F	$\frac{Btu}{hr\,°F}$
18	96	422	326	4670	13.9	369	1394	1210	184	6990	18.8	354	0.96	590	795	1050	352
1	88	439	351	3890	8.95	330	1377	1206	171	7100	19.1	334	1.01	616	838	1030	320
2	94	510	416	2900	5.96	290	1385	1235	150	7040	19.3	290	0.99	680	930	987	296
3	94	580	486	2190	3.88	257	1381	1248	133	6950	19.3	254	0.99	735	994	968	265
19	94	391	297	4750	13.7	342	1373	1159	214	5800	13.5	342	1.00	529	740	1020	335
6	92	435	343	3890	8.80	323	1407	1214	193	5790	13.8	307	0.95	590	834	1030	313
5	95	497	402	2890	5.81	281	1407	1235	172	5790	13.9	274	0.98	641	909	1020	276
4	94	550	456	2190	3.75	242	1368	1227	141	5840	13.9	227	0.94	693	960	962	251
20	97	368	271	4770	13.3	313	1390	1146	244	4520	8.15	303	0.97	489	708	1020	307
7	92	399	307	3890	8.75	289	1403	1184	219	4580	8.50	276	0.95	537	774	1020	283
8	97	466	369	2900	5.78	259	1411	1205	206	4560	8.62	258	0.99	598	859	1030	252
9	98	545	447	2120	3.71	229	1415	1235	180	4530	8.68	224	0.98	659	952	1000	229

TABLE II

Isothermal Pressure Drop Data* on Trane Crossflow Heater (Air Side)

W_a	G_a	$\Delta P_{T_{iso}}$ =	ΔP_{ducts} +	ΔP_{htr}	Calculated	
					ζ_{iso}	$\zeta_{iso} \frac{L}{D}$
(lb/hr)	(lb/hr ft²)	(lb/ft)	(lb/ft²)	(lb/ft²)		
2500	11,600	13.2	3.68	9.52	0.161	3.45
3500	16,200	23.9	7.27	16.6	.139	2.99
5500	25,500	51.8	17.2	34.6	.112	2.40

*Pressure drops obtained from plots of ΔP_a against W_a.

$$\frac{\Delta P_{frict}}{\gamma} = \zeta_{iso} \frac{L}{D} \frac{u_m^2}{2g} \tag{9}$$

$$\frac{\Delta P_{htr}}{\gamma} = \frac{u_m^2}{2g} \left[K_c + \zeta_{iso} \frac{L}{D} + \left(1 - \frac{A_a}{A_3}\right)^2 \right] \tag{11}$$

TABLE III

Isothermal Pressure Drop Data* on Trane Crossflow Heater (Exhaust Gas Side)

W_g	G_g	ΔP_{htr} (meas.)	Calculated		Reynolds number	Predicted
(lb/hr)	(lb/hr ft^2)	(lb/ft^2)	ζ_{iso}	$\zeta_{iso}\frac{L}{D}$	$=\frac{u_m D_g \gamma}{\mu g}$	ζ_{iso}
4000	26,300	11.2	0.0239	0.657	22,000	0.024
6000	39,500	24.1	.0236	.648	33,000	.022
9000	59,200	53.3	.0215	.590	49,700	.020

*Pressure drops obtained from plots of ΔP_g against W_g

$$\frac{\Delta P_{frict}}{\gamma} = \zeta_{iso} \frac{L}{D} \frac{u_m^2}{2g} \tag{9}$$

$$\frac{\Delta P_{htr}}{\gamma} = \frac{u_n^2}{2g}$$

$$\left[\left(\frac{A_g}{A_2}\right)^2 K_c + K + \zeta_{iso}\frac{L}{D} + (1-\eta)\left[1-\left(\frac{A_g}{A_2}\right)^2\right] + \left(\frac{A_g}{A_2}\right)^2\left(1-\frac{A_2}{A_1}\right)^2\right] \tag{12}$$

TABLE IV

Non-Isothermal Pressure Drop Data on Trane Crossflow Heater

Run	W lb/hr	G lb/hr ft^2	Measured isothermal pressure drop*		Predicted non-isothermal pressure drop		Measured non-isothermal pressure drop		T_1	T_2	T_{av}
			$\Delta P_{T_{iso}}$ lb/ft^2 ($T_{iso} = 540^oR$)	$\Delta P'_{T_{iso}}$ in.H_2O	ΔP lb/ft^2	$\Delta P'$ in.H_2O	ΔP lb/ft^2	$\Delta P'$ in.H_2O	^oR	^oR	^oR
					Exhaust Gas Side						
8	4560	34,300	14.3	2.76	43.2	8.32	44.8	8.64	1871	1665	1768
19	5800	43,600	22.6	4.36	65.6	12.6	70.1	13.5	1833	1619	1726
2	7040	52,900	32.7	6.30	108	20.8	100	19.3	1845	1695	1770
					Air Side						
9	2120	9,810	10.2	1.97	17.8	3.43	19.3	3.72	558	1005	781
5	2890	13,400	17.0	3.28	28.7	5.53	30.2	5.82	555	957	756
1	3890	18,000	28.4	5.48	45.9	8.85	46.5	8.96	548	899	724
20	4770	22,100	40.0	7.71	60.1	11.6	68.0	13.1	557	828	693

*These entries are taken from plot of ΔP_g against W_g or ΔP_a against W_a since actual isothermal measurements were at slightly different fluid rates.

$$\Delta P = \Delta P_{T_{iso}} \left(\frac{T_{av}}{T_{iso}}\right)^{1.13} + \left(\frac{G}{3600}\right)^2 \frac{1}{\gamma_1 g}\left(\frac{T_2}{T_1} - 1\right) \qquad (13)$$

$$\Delta P' = \Delta P \times \frac{12}{62.3}, \text{ inches } H_2O$$

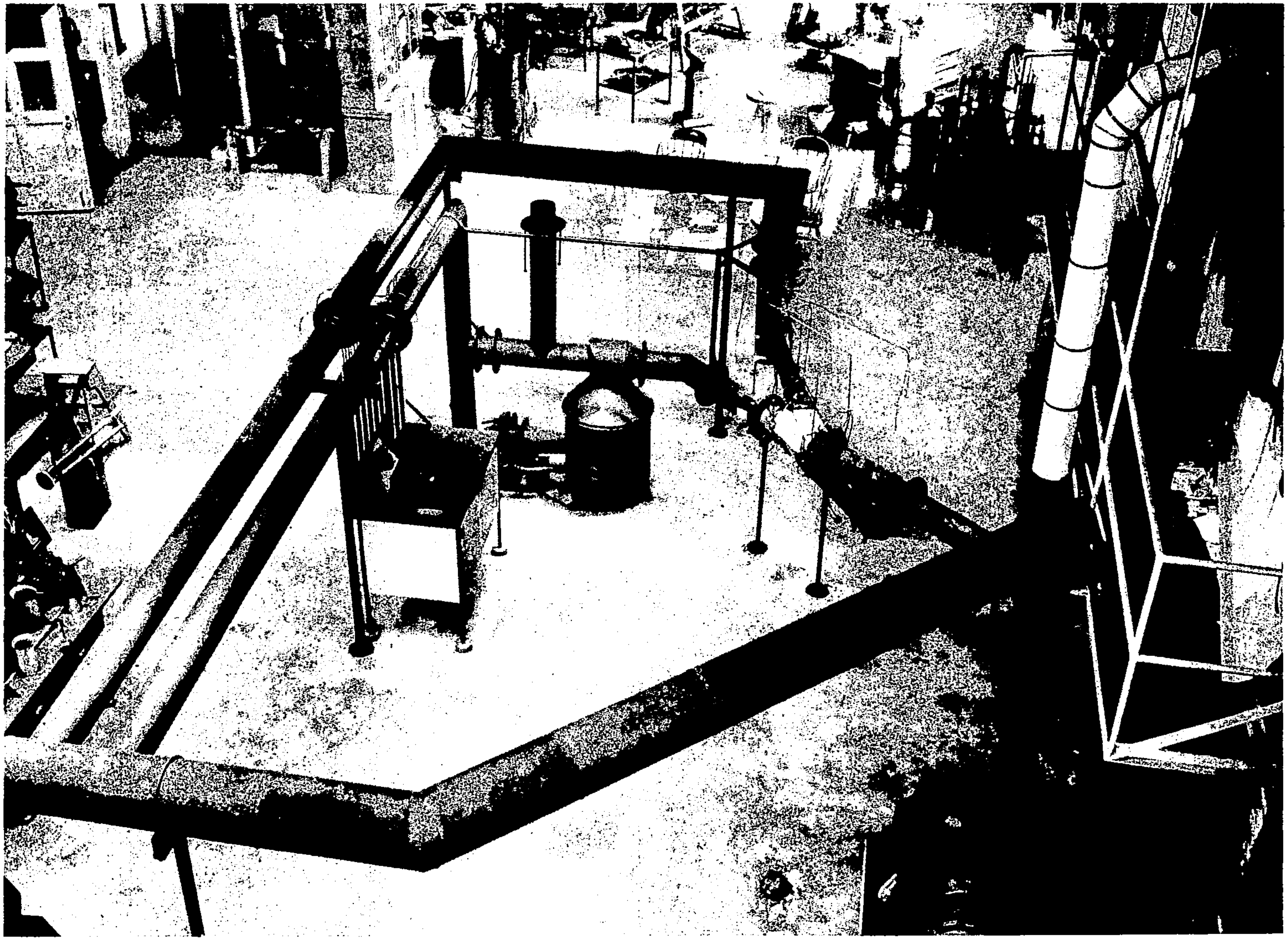

Figure 1.- Photograph of heater test stand.

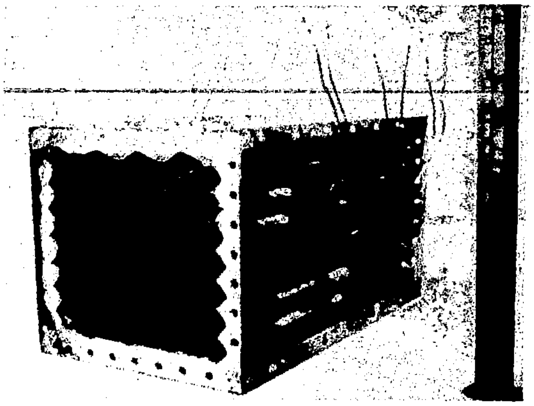

Figure 2.- Photograph of Trane heater.

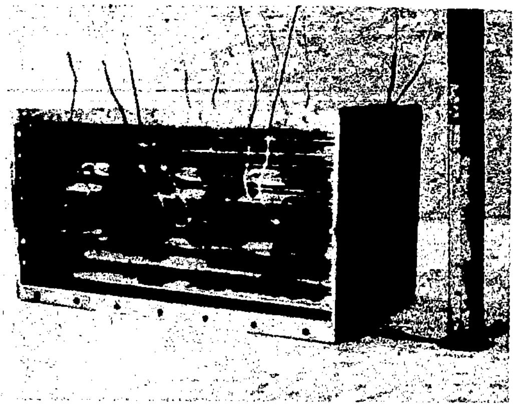

Figure 3.- Photograph of Trane heater.

Figure 4.- Photograph of Trane heater with ventilating-air ducts attached.

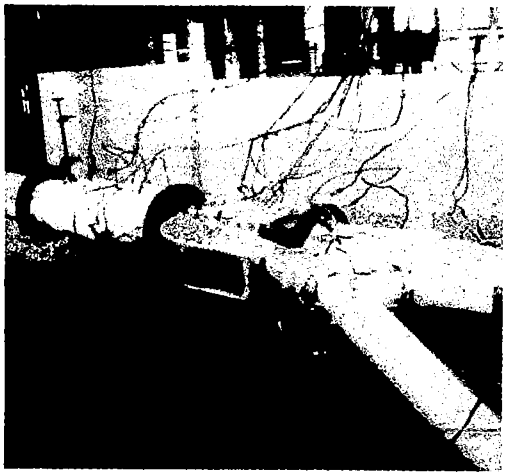

Figure 5.

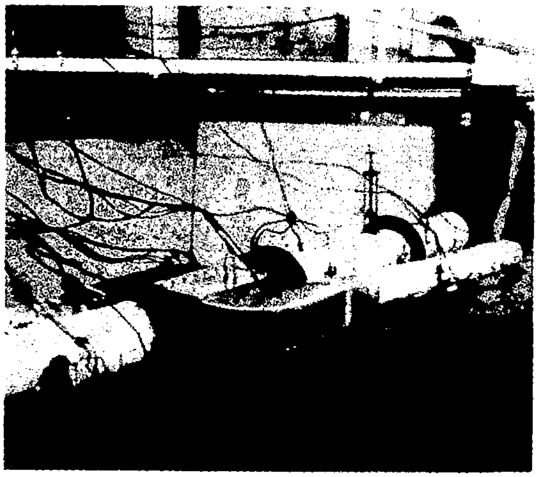

Figure 6.

Figures 5,6.- Photographs of Trane heater installed in test stand.

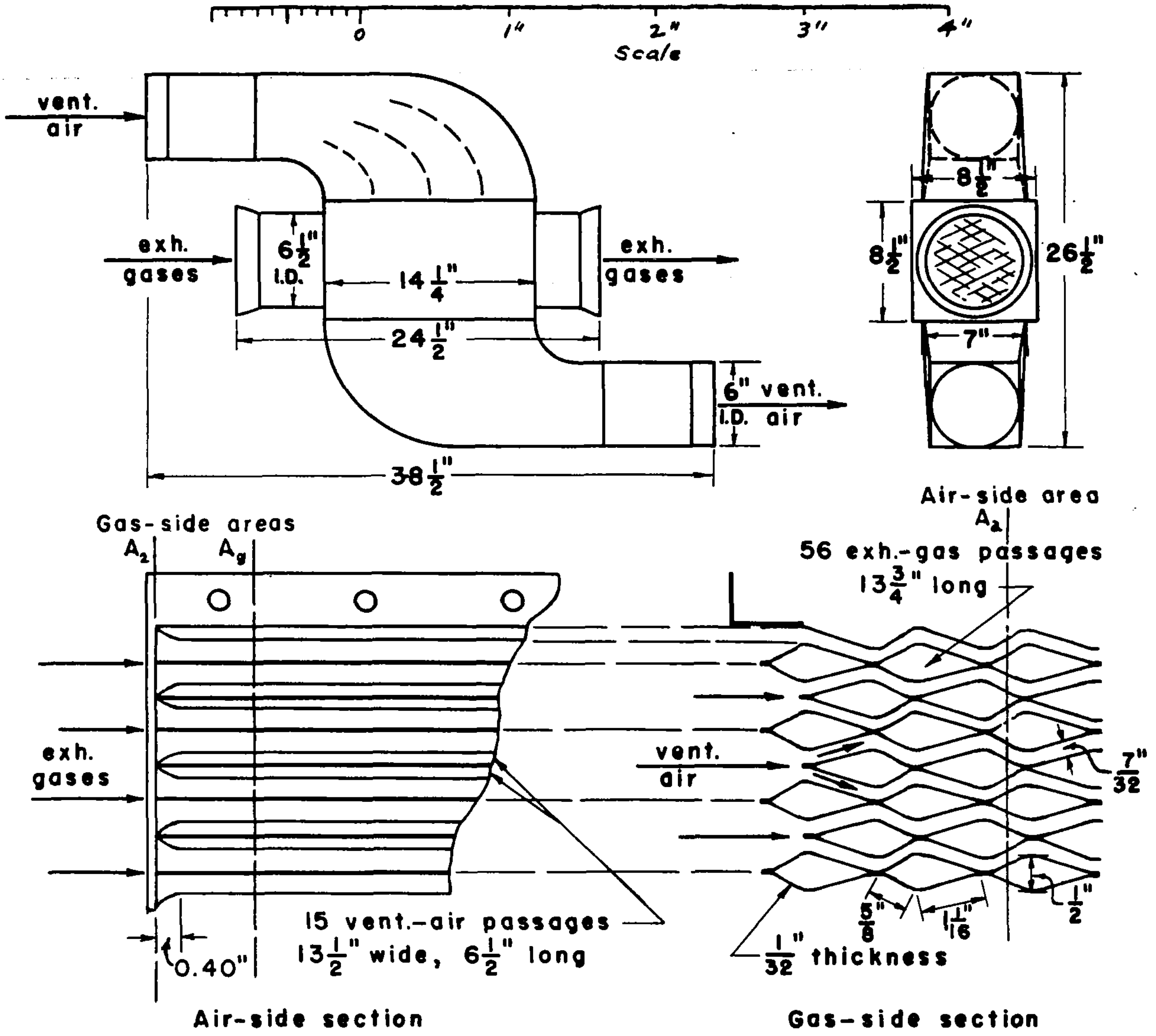

	Air	Gas
Cross section area, ft^2	0.216 (A_a)	0.152 (A_g)
Heat transfer area, ft^2	19.2	19.2
Hydraulic diameter, ft.	0.0253	0.0386

Weight of heater — 33 lbs., shroud — 12 lbs.

Fig. 7 Schematic Diagram of Trane Heater and Air Shroud

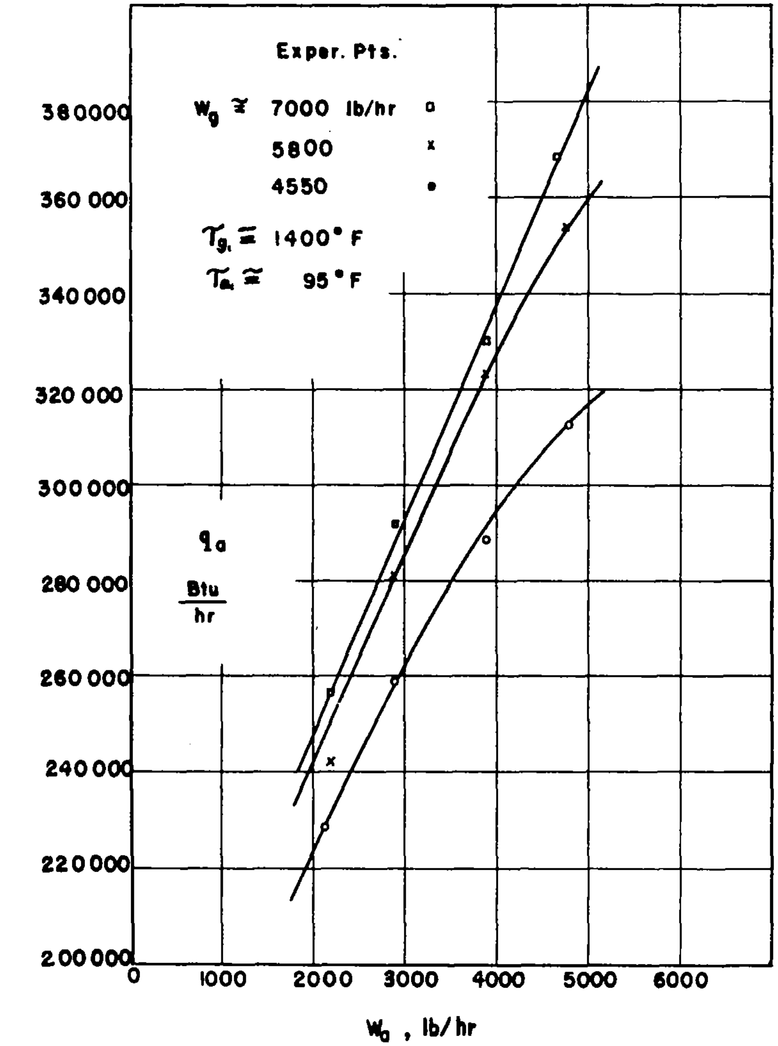

Fig. 8.- Thermal output of Trane exhaust-gas and air heat exchanger as a function of ventilating-air rate

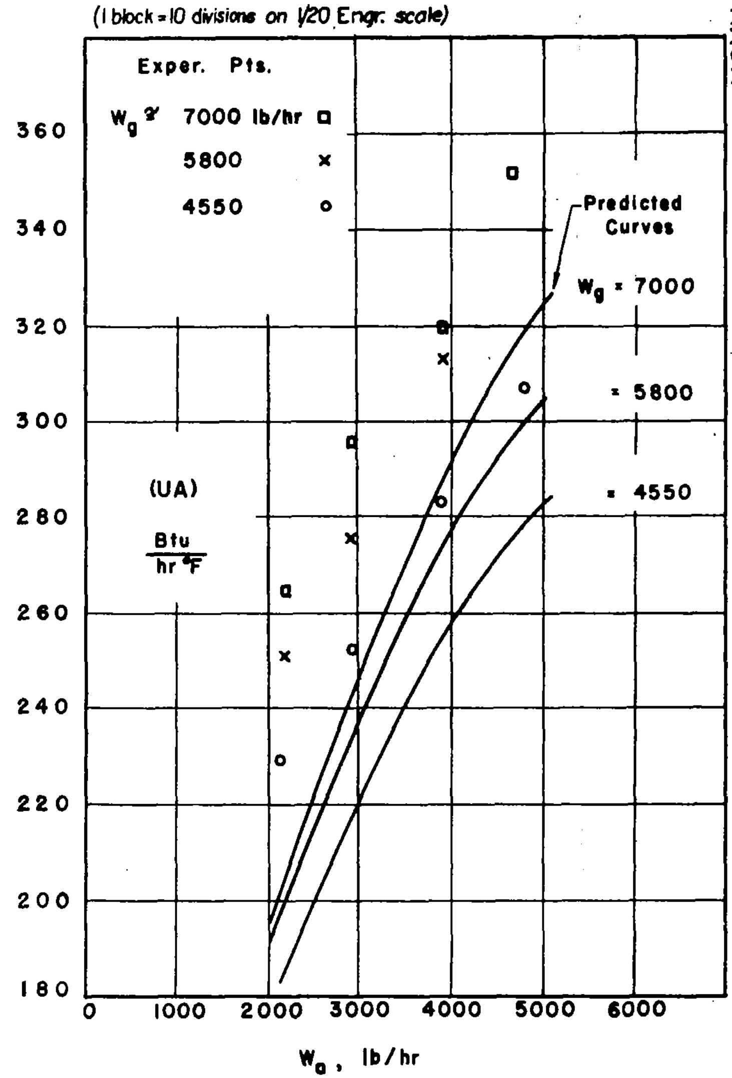

Fig. 9.- Overall conductance of Trane heater as a function of ventilating-air rate.

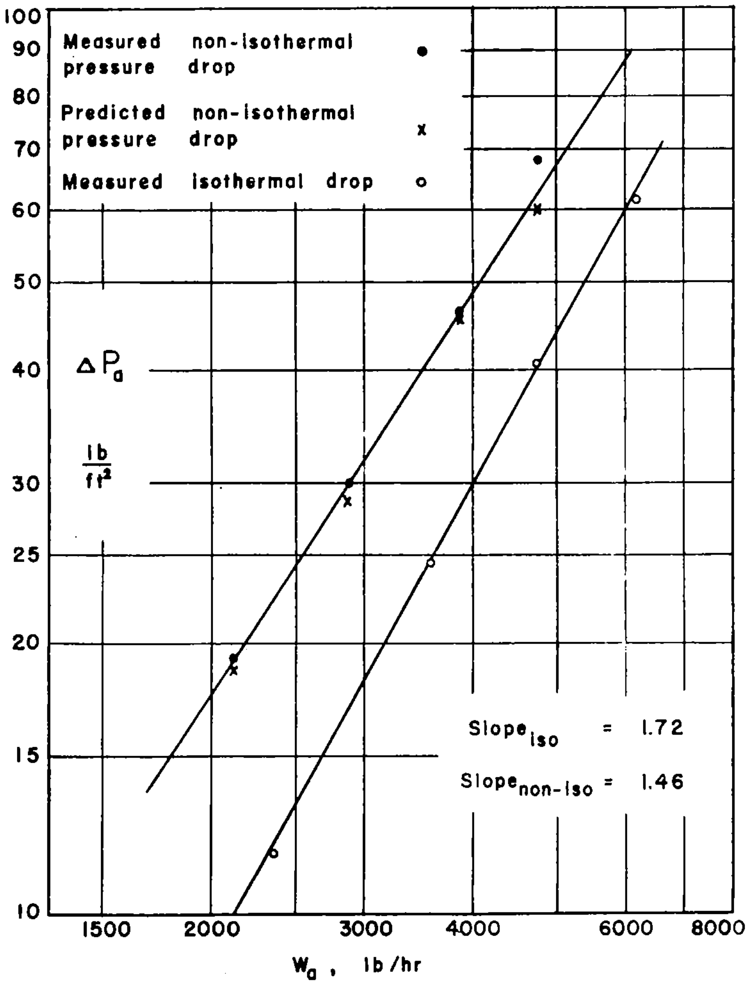

Fig.10.- Pressure drop on air side of Trane heater as a function of ventilating-air rate.

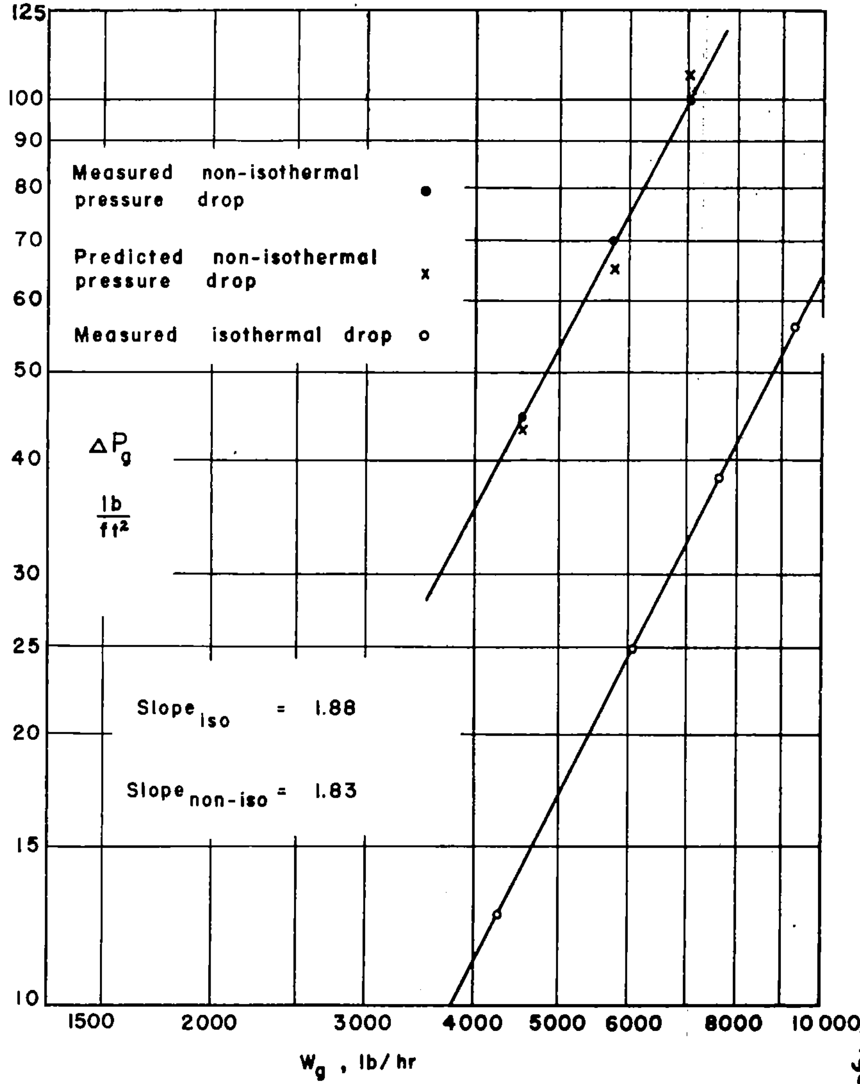

Fig.11.- Pressure drop on exhaust-gas side of Trane heater as a function of exhaust-gas rate.

ATI- 8832
REVISION none
ORIG. AGENCY NO. ARR-3E10
PUBLISHING AGENCY NO.

TITLE: An Investigation of Aircraft Heaters - XII - Performance of a Formed-Plate Crossflow Exhaust Gas and Air Heat Exchanger

AUTHOR(S): Boelter, L. M. K.; Dennison, H. G.; and others

ORIGINATING AGENCY: National Advisory Committee for Aeronautics, Washington, D. C.

PUBLISHED BY: (Same)

DATE	DOC. CLASS.	COUNTRY	LANGUAGE	PAGES	ILLUSTRATIONS
May '43	Unclass.	U.S.	Eng.	24	photos, tables, diagrs, graphs

ABSTRACT:

Heat exchanger was performance tested using exhaust gas rates from 4550 to 7000 lb/hr and ventilating air rates from 2200 to 4750 lb/hr. At exhaust gas rate of 5800 lb/hr and air rate of 3000 lb/hr, thermal output was 285,000 BTU/hr and pressure drops were 6.2 in. water on air side and 14 in. on exhaust gas side. Pressure drop on exhaust gas side may possibly be reduced by decreasing cross-section area restriction and yet not greatly reducing thermal output.

DISTRIBUTION: Request copies of this report only from Originating Agency

DIVISION: Comfortization (23)
SECTION: Air Conditioning (1)

SUBJECT HEADINGS: Heaters, Aircraft (49000); Heat exchangers (48400)

ATI SHEET NO.: R-23-1-13

UNCLASSIFIED PER AUTHORITY INDEX
OF NACA TECHNICAL PUBLICATIONS
DATED 31 DECEMBER 1947.

p1/3, p13/1

Fld 23

*Aircraft heaters
Heat exchangers